NASA/TM–2007–214882

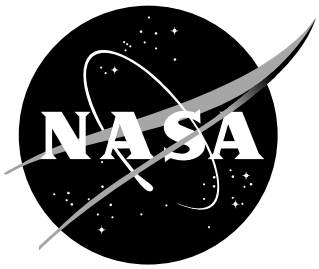

Orbiter Entry Aeroheating Working Group viscous CFD boundary layer transition trailblazer solutions

William A. Wood, David W. Erickson, and Francis A. Greene
Langley Research Center, Hampton, Virginia

June 2007

The NASA STI Program Office ... in Profile

Since its founding, NASA has been dedicated to the advancement of aeronautics and space science. The NASA Scientific and Technical Information (STI) Program Office plays a key part in helping NASA maintain this important role.

The NASA STI Program Office is operated by Langley Research Center, the lead center for NASA's scientific and technical information. The NASA STI Program Office provides access to the NASA STI Database, the largest collection of aeronautical and space science STI in the world. The Program Office is also NASA's institutional mechanism for disseminating the results of its research and development activities. These results are published by NASA in the NASA STI Report Series, which includes the following report types:

- TECHNICAL PUBLICATION. Reports of completed research or a major significant phase of research that present the results of NASA programs and include extensive data or theoretical analysis. Includes compilations of significant scientific and technical data and information deemed to be of continuing reference value. NASA counterpart of peer-reviewed formal professional papers, but having less stringent limitations on manuscript length and extent of graphic presentations.
- TECHNICAL MEMORANDUM. Scientific and technical findings that are preliminary or of specialized interest, e.g., quick release reports, working papers, and bibliographies that contain minimal annotation. Does not contain extensive analysis.
- CONTRACTOR REPORT. Scientific and technical findings by NASA-sponsored contractors and grantees.
- CONFERENCE PUBLICATION. Collected papers from scientific and technical conferences, symposia, seminars, or other meetings sponsored or co-sponsored by NASA.
- SPECIAL PUBLICATION. Scientific, technical, or historical information from NASA programs, projects, and missions, often concerned with subjects having substantial public interest.
- TECHNICAL TRANSLATION. English-language translations of foreign scientific and technical material pertinent to NASA's mission.

Specialized services that complement the STI Program Office's diverse offerings include creating custom thesauri, building customized databases, organizing and publishing research results ... even providing videos.

For more information about the NASA STI Program Office, see the following:

- Access the NASA STI Program Home Page at ***http://www.sti.nasa.gov***
- E-mail your question via the Internet to help@sti.nasa.gov
- Fax your question to the NASA STI Help Desk at (301) 621–0134
- Phone the NASA STI Help Desk at (301) 621–0390
- Write to:
  NASA STI Help Desk
  NASA Center for AeroSpace Information
  7115 Standard Drive
  Hanover, MD 21076–1320

NASA/TM–2007–214882

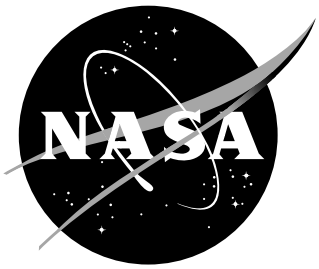

Orbiter Entry Aeroheating Working Group viscous CFD boundary layer transition trailblazer solutions

William A. Wood, David W. Erickson, and Francis A. Greene
Langley Research Center, Hampton, Virginia

National Aeronautics and
Space Administration

Langley Research Center
Hampton, Virginia 23681-2199

June 2007

The use of trademarks or names of manufacturers in this report is for accurate reporting and does not constitute an offical endorsement, either expressed or implied, of such products or manufacturers by the National Aeronautics and Space Administration.

Available from:

NASA Center for AeroSpace Information (CASI)
7115 Standard Drive
Hanover, MD 21076–1320
(301) 621–0390

National Technical Information Service (NTIS)
5285 Port Royal Road
Springfield, VA 22161–2171
(703) 605–6000

Abstract

Boundary layer transition correlations for the Shuttle Orbiter have been previously developed utilizing a two-layer boundary layer prediction technique. The particular two-layer technique that was used is limited to Mach numbers less than 20. To allow assessments at Mach numbers greater than 20, it is proposed to use viscous CFD to the predict boundary layer properties. This report addresses if the existing Orbiter entry aeroheating viscous CFD solutions, which were originally intended to be used for heat transfer rate predictions, adequately resolve boundary layer edge properties and if the existing two-layer results could be leveraged to reduce the number of needed CFD solutions. The boundary layer edge parameters from viscous CFD solutions are extracted along the wind side centerline of the Space Shuttle Orbiter at reentry conditions, and are compared with results from the two-layer boundary layer prediction technique. The differences between the viscous CFD and two-layer prediction techniques vary between Mach 6 and 18 flight conditions and Mach 6 wind tunnel conditions, and there is not a straightforward scaling between the viscous CFD and two-layer values. Therefore: it is not possible to leverage the existing two-layer Orbiter flight boundary layer data set as a substitute for a viscous CFD data set; but viscous CFD solutions at the current grid resolution are sufficient to produce a boundary layer data set suitable for applying edge-based boundary layer transition correlations.

Nomenclature

Symbols

H	total enthalpy, BTU/slug
L	reference length; 1280 in. full-scale, 9.6 in. wind tunnel model scale
M	Mach number
Re	Reynolds number
Re_θ	$V_e\theta/\nu_e$
V	fluid speed, fps
δ	boundary layer thickness, in.
μ	viscosity, slug/ft-s
ν	kinematic viscosity, μ/ρ, ft^2/s
ρ	density, $slug/ft^3$
θ	momentum thickness, in.

Subscripts

e	boundary layer edge
inv	inviscid layer
∞	free stream

Acronyms

CFD	computational fluid dynamics

ISSHVFW	International Space Station heavy vehicle forward weight
RTF	return-to-flight
STS	space transportation system

Introduction

This report is a formal product delivery from Langley Research Center to the Space Shuttle program in support of the return-to-flight (RTF) effort, as specified in a sub-task agreement, number RTF-08, between Langley and Johnson Space Center. The scope of the work is set by the sub-task agreement.

The technology addressed is the numerical prediction of boundary layer edge properties in the flow about the Shuttle Orbiter at reentry and hypersonic wind tunnel conditions. The engineering context is the development and application of boundary layer transition predictions for the Orbiter during reentry, in particular for the prediction of forced, or bypass, transition due to an off-nominal Orbiter wind side surface.

Previously, a data set of boundary layer properties used to correlate boundary layer transition behavior for the Orbiter at both wind tunnel and flight conditions had been created using a two-layer technique [2]. The two-layer technique uses computational fluid dynamics (CFD) to predict an inviscid flow field and then utilizes an approximate engineering tool to account for the effect of viscosity, producing the boundary layer estimates. Boundary layer transition correlations [1] have been created for the Orbiter program recently using this wind tunnel data set in conjunction with wind tunnel experiments, and the correlations are applied as part of the Shuttle mission operations.

There is a shortcoming in the current transition prediction tool that motivates the present study: the existing two-layer technique does not account for non-equilibrium chemistry. Chemical non-equilibrium effects are important in the Orbiter reentry flow field at Mach numbers greater than 15–18 [8], but boundary layer transition predictions are desired up to Mach 21–23.

The viscous CFD codes used by the Orbiter Entry Aeroheating Team model chemical non-equilibrium and are suitable for simulating all Mach number Orbiter flow fields within the continuum regime, up to about Mach 25, and thus could alleviate the shortcoming. This report investigates the feasibility of using the viscous CFD solvers instead of the two-layer engineering approach to define the Orbiter boundary layer properties from which new boundary layer transition correlations may be developed. While not investigated in the present study, viscous CFD flow field simulations also provide boundary layer profile data, which the two-layer technique does not. Having boundary layer profile data may allow the development of transition correlations that are not possible in the two-layer context. The moniker trailblazer is used to reflect the feasibility nature of this study, in contrast to subsequent work to develop the full flight database.

The viscous CFD codes used for the present study have been shown [4] to match measured boundary layer thickness for an Orbiter model at wind tunnel conditions with an 11% standard deviation. For this trailblazer report, 11% is used as an

acceptance criteria.

If the existing two-layer results could be scaled or otherwise mapped to match viscous CFD results, then conversion to viscous CFD correlations would only require new high-Mach-number flight solutions. Otherwise, a full viscous CFD data set would have to be generated at both flight and wind tunnel conditions. The primary task of this report is to spot check the two-layer and viscous CFD boundary layer properties for equivalence or a simple scaling relationship. Two ancillary questions addressed in the report are the adequacy of grid resolution in the viscous CFD solutions and the consistency between LAURA and DPLR results.

CFD codes

The two-layer boundary layer prediction technique used the Langley Approximate Three-Dimensional Convective Heating engineering code (LATCH [3]) to provide the boundary layer properties. LATCH requires a background inviscid CFD solution within which to operate. The inviscid flow fields for the two-layer technique are provided by the Langley Aerothermodynamic Upwind Relaxation Algorithm (LAURA [5, 6]). LAURA is a nominally second-order accurate upwind finite-volume flow solver with a five-species, single-temperature air model.

LAURA is also used as a viscous flow solver, along with the Data-Parallel Line Relaxation code (DPLR [7]), to compute boundary layers integral to the flow field simulations. Both LAURA and DPLR are used with a five-species, single-temperature air model, a partially catalytic surface with reaction-cured glass properties, and a radiative equilibrium surface temperature with an emissivity of 0.89. Both LAURA and DPLR have been accepted by the Orbiter Configuration Control Board for the simulation of smooth-body laminar Orbiter entry flow fields [4].

Boundary layer edge definition

The boundary layer edge is determined from the CFD solutions using the BLAYER [4, 9] post-processing software. Within BLAYER, the boundary layer edge is defined as the distance above the surface where $H = 0.995\, H_{inv}$. In general, $H_{inv} = H_\infty$, but the BLAYER detection logic is designed to accommodate locations within the CFD solutions where total enthalpy is not exactly conserved through the bow shock due to numerical dissipation effects.

Grid convergence

Grid convergence of the predicted transition parameter was investigated by refining the CFD volume grids in the direction traversing from the Orbiter surface to the free stream. The primary boundary layer transition parameter utilized by RTF can be expressed as $\left(\frac{Re_\theta}{M_e}\right)\cdot\left(\frac{1}{\delta}\right)$. The symbols have conventional meaning: δ is boundary layer thickness, M_e is boundary layer edge Mach number, and Re_θ is Reynolds number based on momentum thickness.

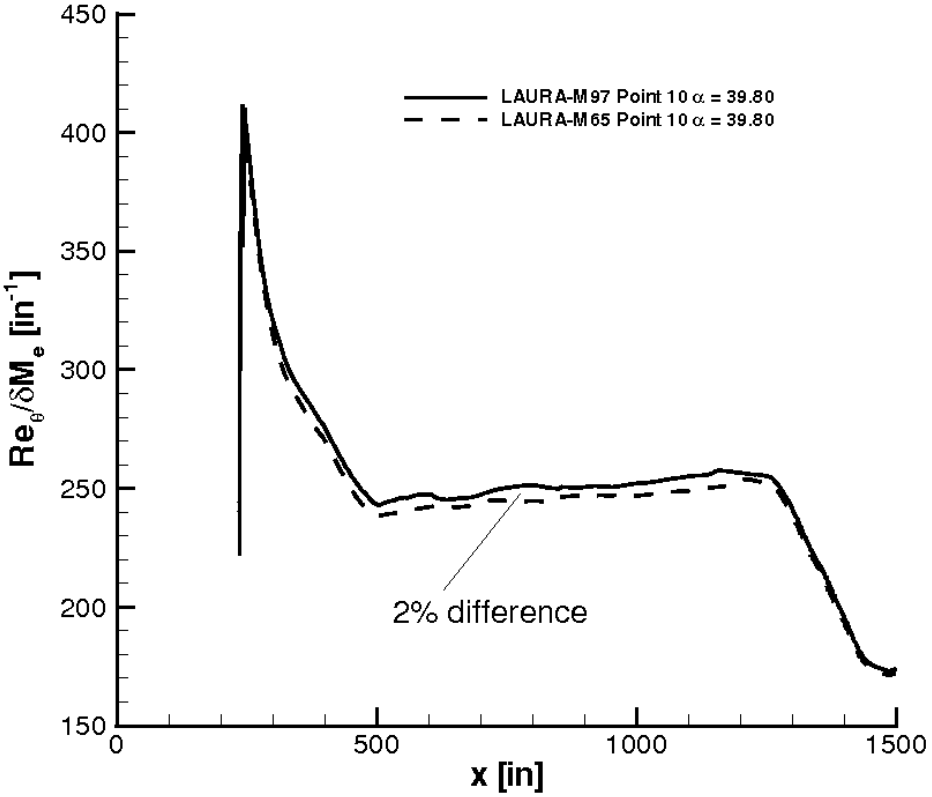

Figure 1. Grid convergence of $\left(\frac{Re_\theta}{M_e}\right)\cdot\left(\frac{1}{\delta}\right)$ at Mach 12. Fine grid (M 97) has 97 points, versus 65 for coarse (M 65), in the body-normal direction.

The grid convergence of the transition parameter $\left(\frac{Re_\theta}{M_e}\right)\cdot\left(\frac{1}{\delta}\right)$ along the Orbiter wind side centerline is shown in Figure 1 at Mach 12 flight conditions and in Figure 2 at Mach 18 flight conditions. The Mach 12 case corresponds to a point on the ISSHVFW [4] trajectory. The Mach 18 case is at the same free stream conditions as an STS-107 trajectory point but is at 45 degrees angle of attack. All solutions are viscous LAURA solutions. The legend designation 'M65' indicates solutions with 65 points in the body-normal direction, shown as dashed lines in the figures.The fine grids, 'M97', have 50% more cells, for 97 points in the body-normal direction. The largest differences between the solutions are 2% at Mach 12 and 4% at Mach 18.

Flight boundary layers

Consistency comparisons of predicted boundary layer properties from LAURA, DPLR, and LATCH were performed for one point on the ISSHVFW trajectory (Mach 6, Figures 3–5) and two points on the STS-107 trajectory (Mach 18, Figures 6–8; and Mach 20, Figures 9–11). The comparisons seek to identify similarities or trends between the viscous-CFD and two-layer results for boundary layer thickness, Re_θ/M_e,

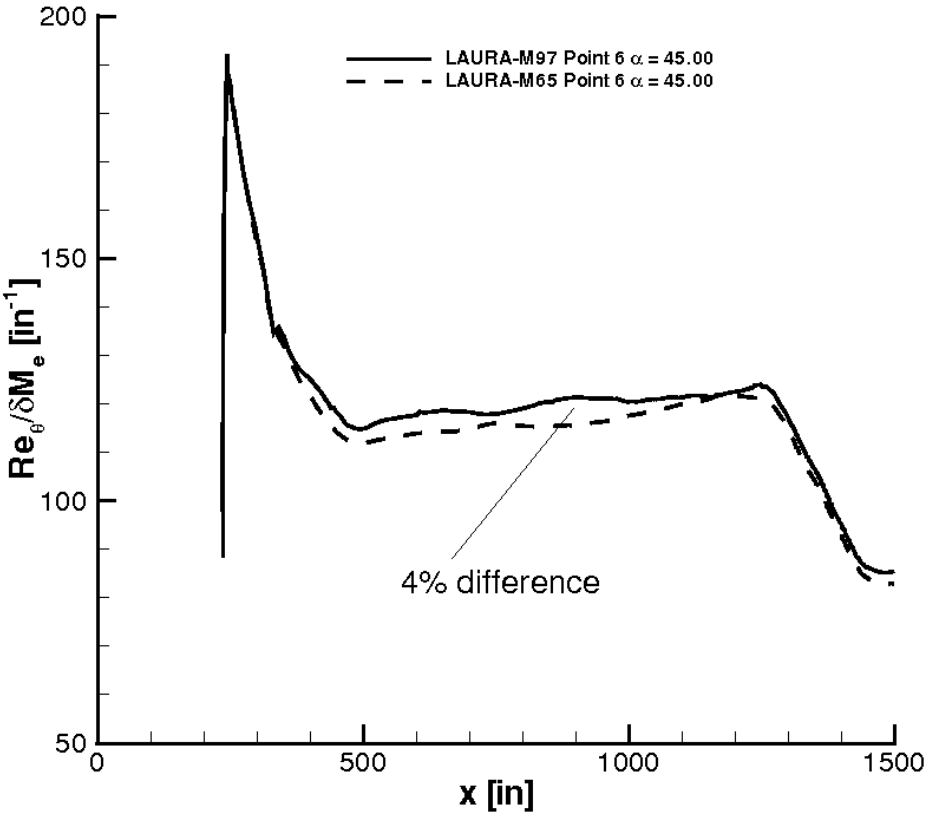

Figure 2. Grid convergence of $\left(\frac{Re_\theta}{M_e}\right)\cdot\left(\frac{1}{\delta}\right)$ at Mach 18. Fine grid (M 97) has 97 points, versus 65 for coarse (M 65), in the body-normal direction.

and $\left(\frac{Re_\theta}{M_e}\right)\cdot\left(\frac{1}{\delta}\right)$. All the comparisons depict wind-side centerline data extractions from the full vehicle solutions.

Boundary layer thickness results for the Orbiter wind side centerline are shown in Figure 3, at Mach 6, Figure 6, at Mach 18, and Figure 9, at Mach 20 flight conditions. For flight cases, the LATCH boundary layer thickness is determined from the momentum thickness based upon a shape factor [10] related to the wall-to-total enthalpy ratio. At Mach 6 the largest difference between the LAURA and LATCH solutions is 19%. At Mach 18 the agreement is better, with a maximum difference of 8%. The LAURA and DPLR solutions differ by less than 5% for both Mach 18 and Mach 20.

Figures 4, 7, and 10 show the corresponding Re_θ/M_e results. There is considerable disagreement for LAURA and LATCH results for both Mach 6 and Mach 18: 17% maximum difference for Mach 6 and larger differences along nearly the entire profile for Mach 18. The agreement between LAURA and DPLR results is better, with only 8% maximum differences at Mach 18 and 11% at Mach 20.

The results for $\left(\frac{Re_\theta}{M_e}\right)\cdot\left(\frac{1}{\delta}\right)$ at Mach 6, Mach 18, and Mach 20 are presented in Figures 5, 8, and 11, respectively. For Mach 6 the discrepancies in boundary layer thickness and Re_θ/M_e for LAURA and LATCH counteract one another so that

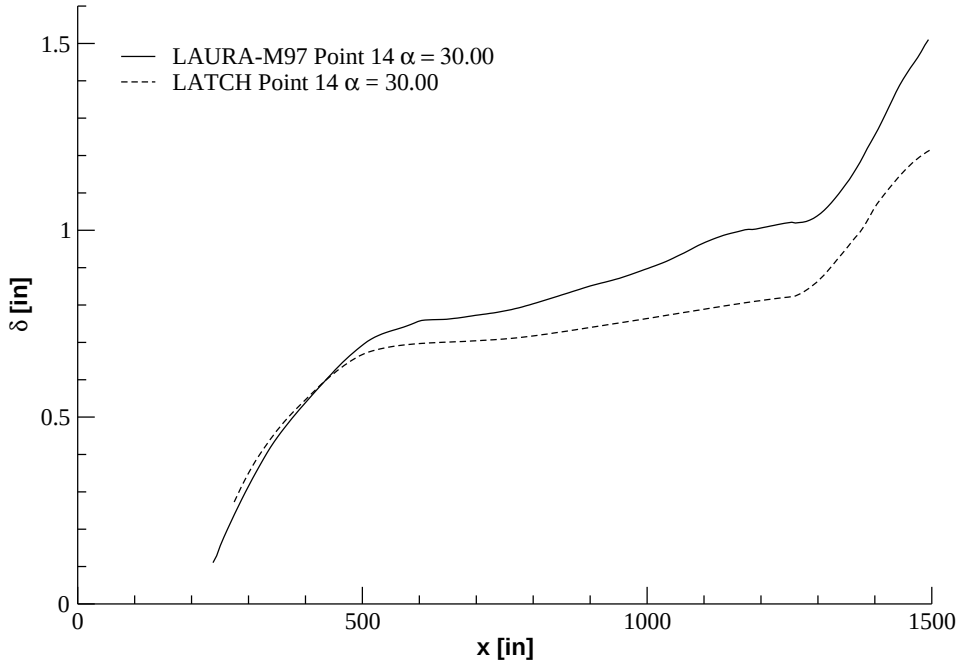

Figure 3. LAURA-LATCH centerline boundary layer thickness, Mach 6 flight.

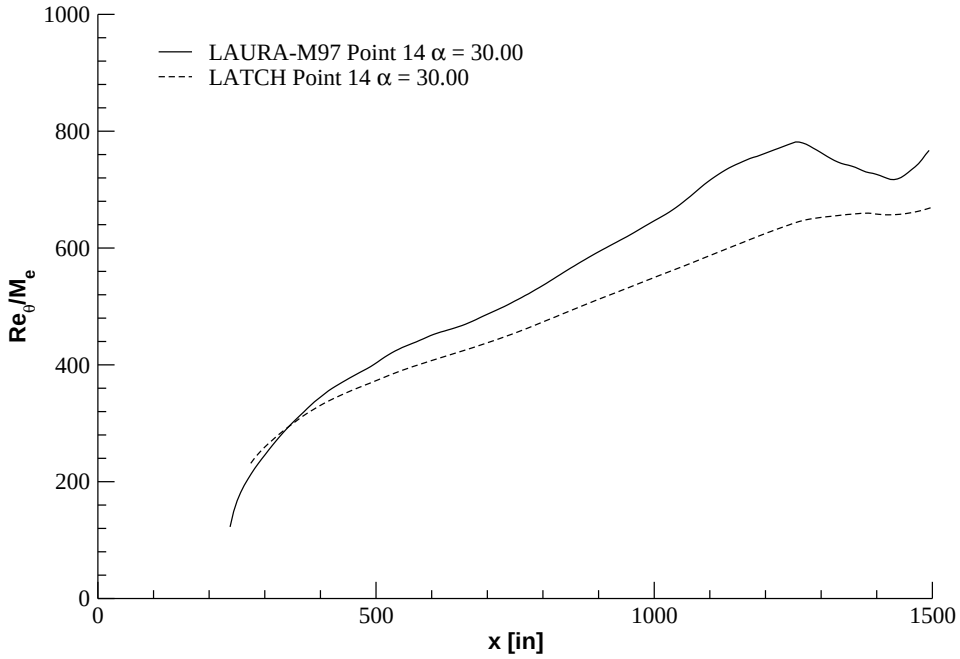

Figure 4. LAURA-LATCH Re_θ/M_e, Mach 6 flight wind side centerline.

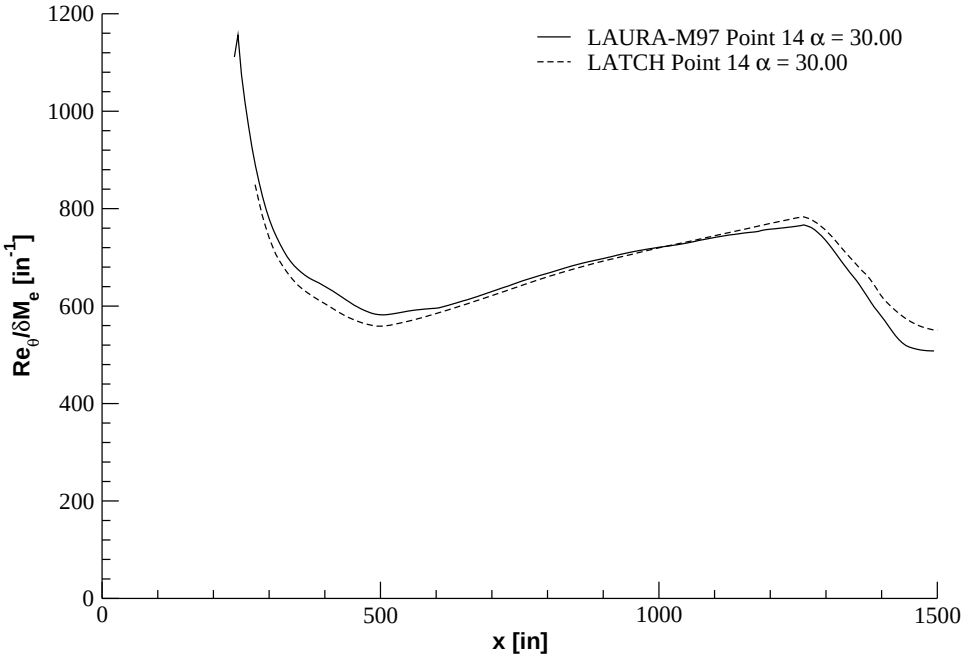

Figure 5. LAURA-LATCH $\left(\frac{Re_\theta}{M_e}\right)\cdot\left(\frac{1}{\delta}\right)$, Mach 6 flight wind side centerline.

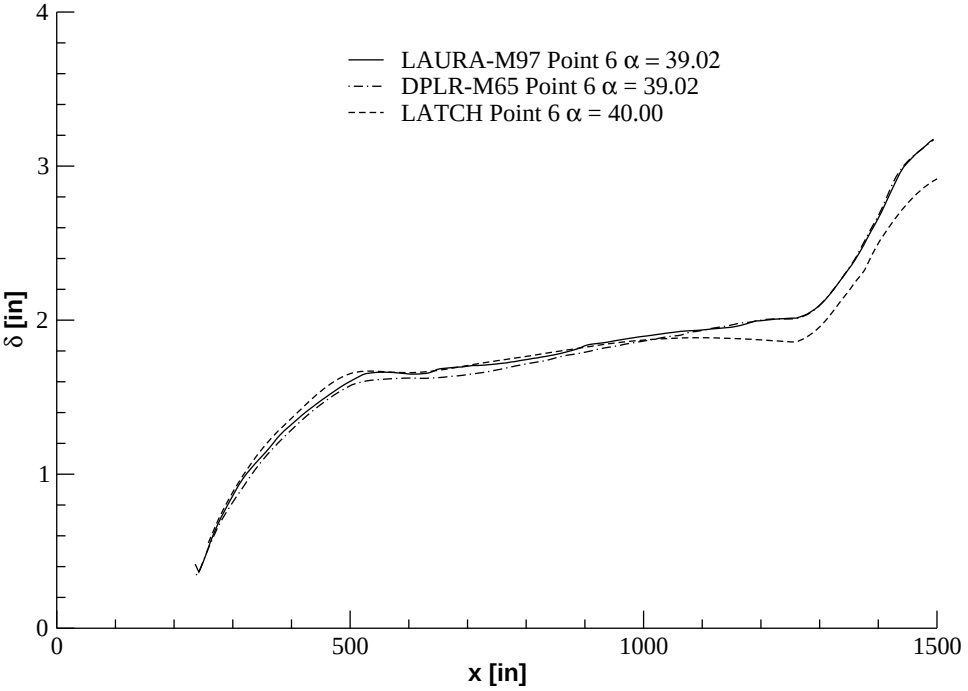

Figure 6. LAURA, DPLR, and LATCH centerline boundary layer thickness, Mach 18 flight.

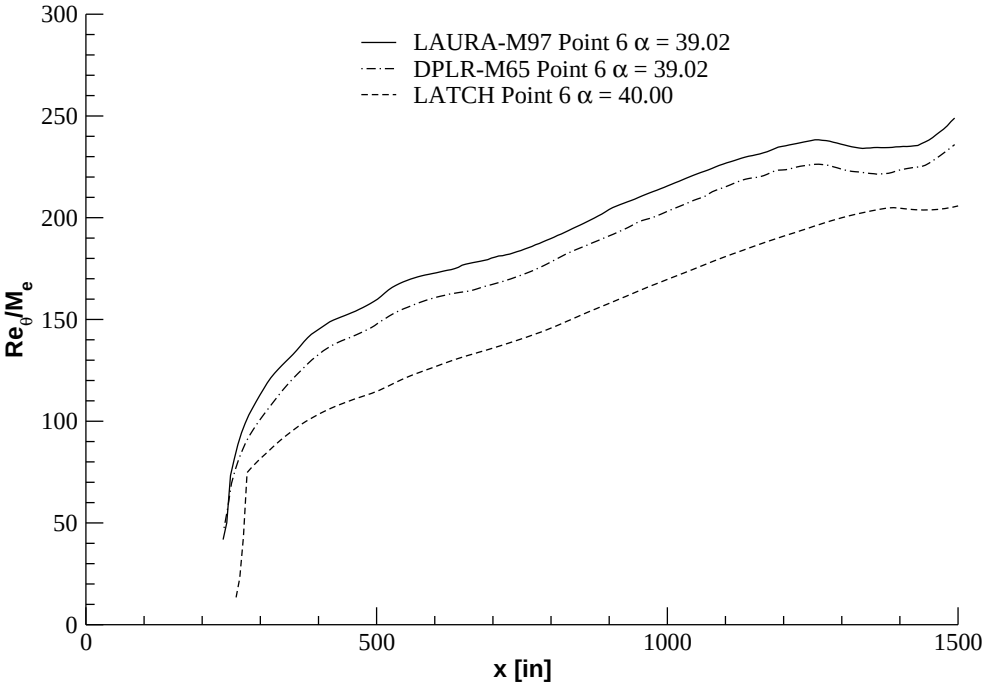

Figure 7. LAURA, DPLR, and LATCH centerline Re_θ/M_e, Mach 18 flight.

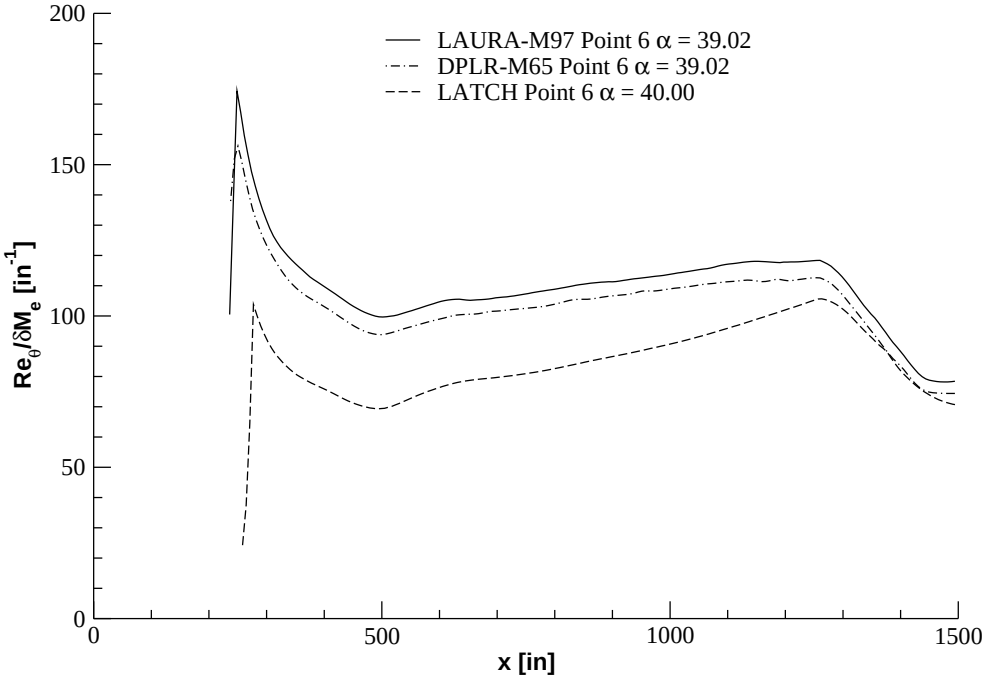

Figure 8. LAURA, DPLR, and LATCH centerline $\left(\frac{Re_\theta}{M_e}\right)\cdot\left(\frac{1}{\delta}\right)$, Mach 18 flight.

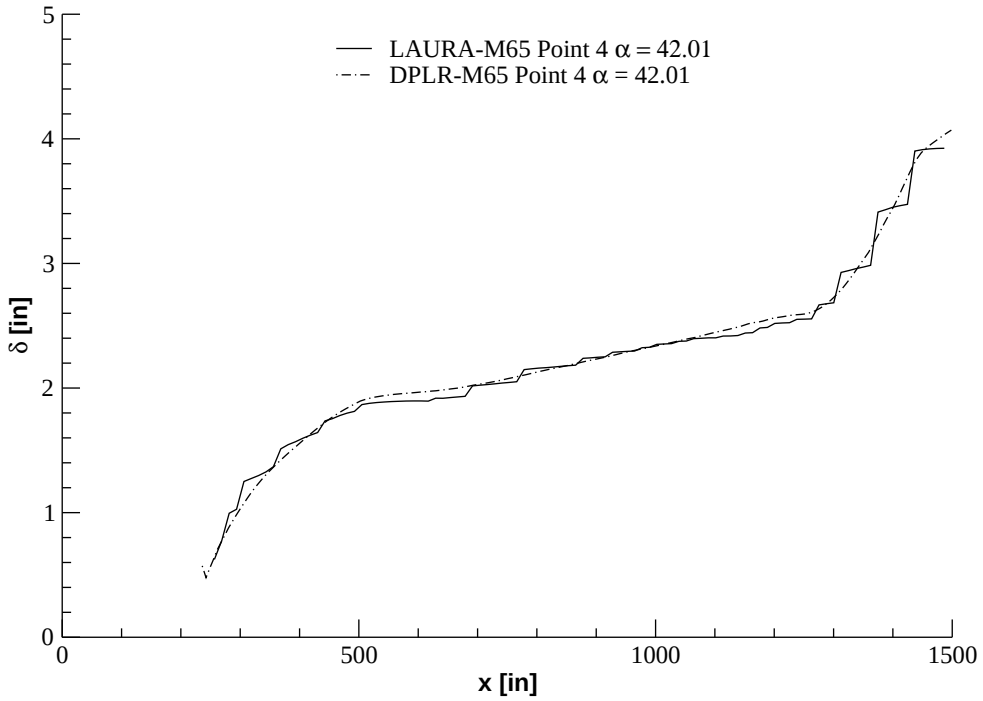

Figure 9. LAURA-DPLR centerline boundary layer thickness, Mach 20 flight.

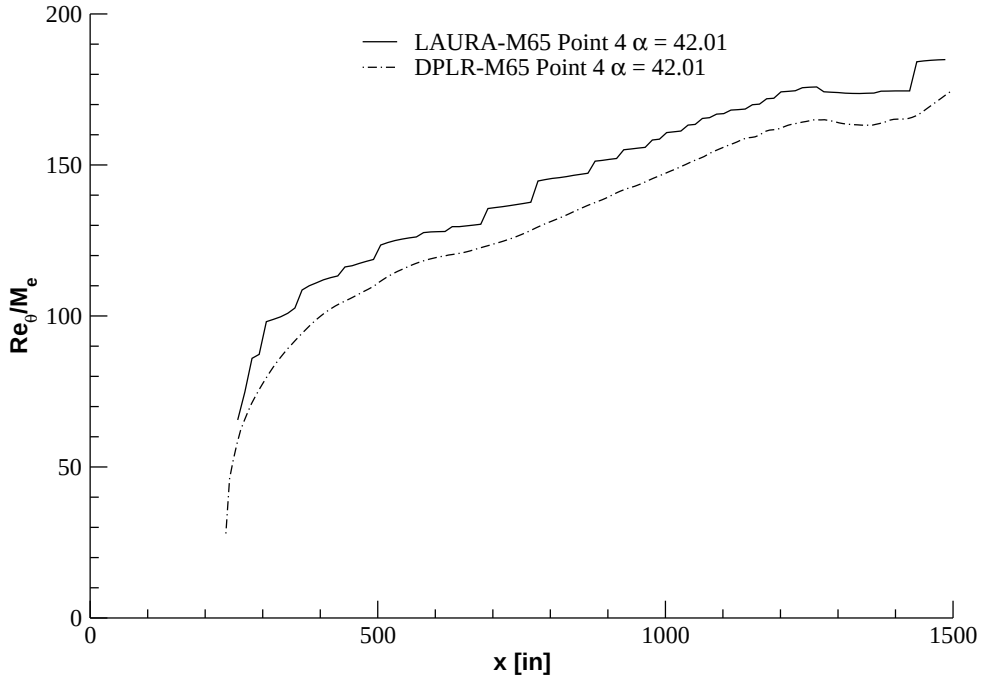

Figure 10. LAURA-DPLR Re_θ/M_e, Mach 20 flight wind side centerline.

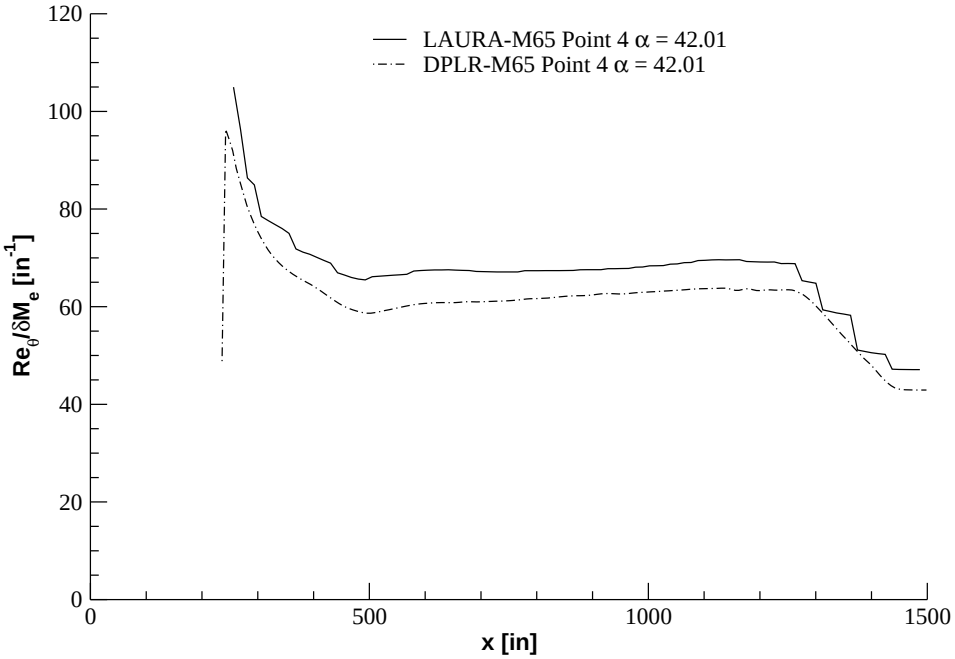

Figure 11. LAURA-DPLR $\left(\frac{Re_\theta}{M_e}\right)\cdot\left(\frac{1}{\delta}\right)$, Mach 20 flight wind side centerline.

$\left(\frac{Re_\theta}{M_e}\right)\cdot\left(\frac{1}{\delta}\right)$ is in close agreement. At Mach 18, however, the results do not agree nearly as well. A simple relation between the LATCH and LAURA boundary layer properties is not apparent for these flight conditions. LAURA and DPLR results agree much better at Mach 18 with maximum differences of only 6%. The agreement at Mach 20 has maximum differences of 11%.

The results shown here were drawn from the viscous CFD flight data set. In the current viscous flight data set, solutions were produced using LAURA for $M \leq 20$ and are a mixture of LAURA and DPLR results for higher Mach numbers.

Wind tunnel boundary layers

The boundary layer transition correlations are applied using the flight predicted boundary layer properties. The correlations are developed using boundary layer property predictions at wind tunnel conditions corresponding to wind tunnel boundary layer trip experiments. LAURA and LATCH boundary layer thicknesses, Figure 12, and Re_θ/M_e, Figure 13, on the wind side centerline are compared for consistency on a 0.75%-scale Orbiter model at Mach 6 wind tunnel conditions. For wind tunnel simulations, the LATCH code relates the boundary layer thickness to the momentum thickness using a constant shape factor, equal to 7.5.

Comparing Mach-6 results in Figures 12 (tunnel) and 14 (flight—repetition of Figure 3 for convenience) the agreement in boundary layer thickness is different for the tunnel than at flight. Both prediction methods agree on the nose cap at both tunnel and flight, up to the 500 inch station in Figure 3 and up to 20% of the body

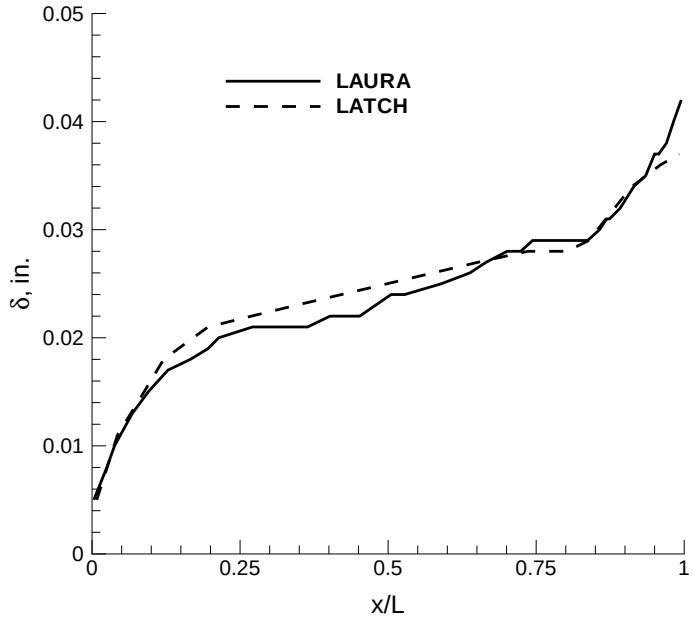

Figure 12. LAURA-LATCH boundary layer thickness comparison, Mach 6 wind tunnel wind side centerline.

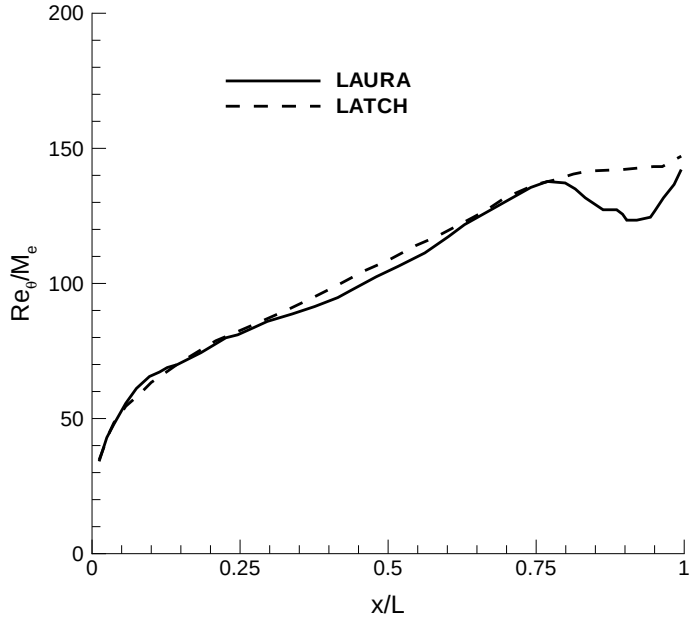

Figure 13. LAURA-LATCH Re_θ/M_e comparison, Mach 6 wind tunnel wind side centerline.

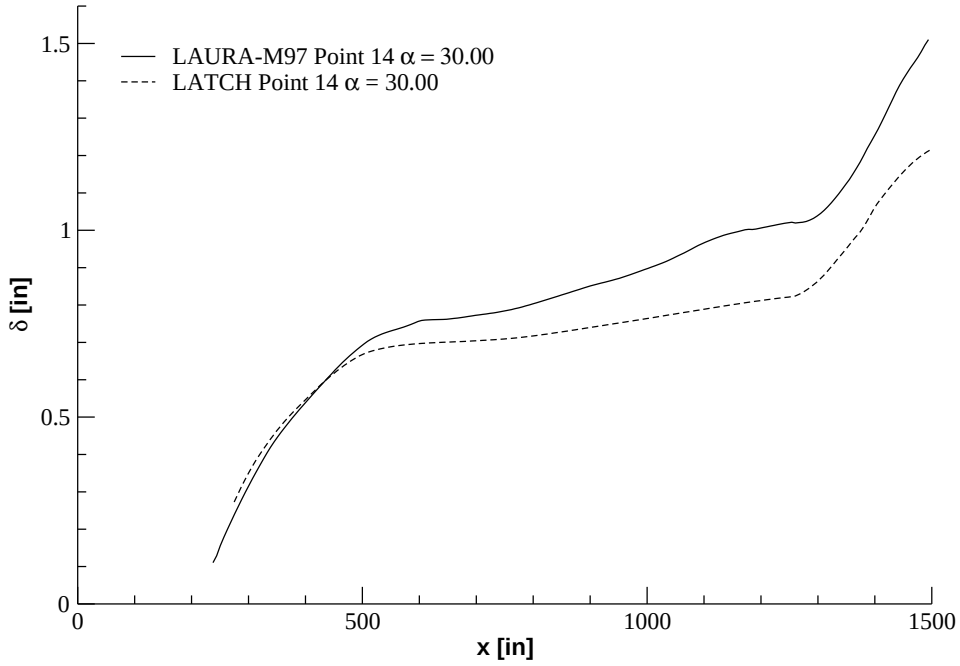

Figure 14. LAURA-LATCH centerline boundary layer thickness, Mach 6 flight.

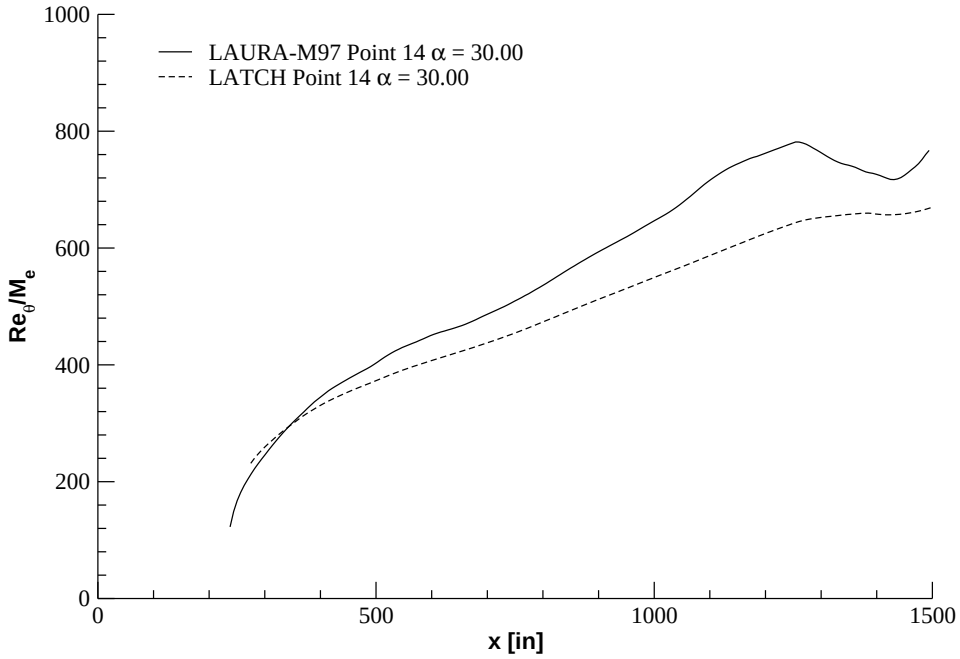

Figure 15. LAURA-LATCH Re_θ/M_e, Mach 6 flight wind side centerline.

length in Figure 12. But the LAURA boundary layer distribution down the remainder of the centerline is similar between the tunnel and flight conditions. In contrast, the LATCH flight boundary layer thickness grows more slowly with running length at flight than at tunnel conditions. As a result, the LAURA and LATCH boundary layer thicknesses agree at tunnel conditions but have as much as 19% differences at flight. Thus a boundary layer transition correlation developed from the wind tunnel boundary layer thickness data would produce different transition onset predictions when applied at flight conditions, depending upon whether the LATCH or the LAURA flight data sets were used.

The same trends apply to Re_θ/M_e as for the boundary layer thickness, shown along the wind side centerline in Figures 13 (tunnel) and 15 (flight—repetition of Figure 4 for convenience). The LAURA and LATCH results are in agreement over the fore 80% of the vehicle at tunnel conditions. At flight, the LAURA and LATCH results are in agreement on the nose cap, but the LATCH results rise more slowly with running length than the LAURA data, with a maximum 17% difference. Again, a boundary layer transition correlation developed from the wind tunnel Re_θ/M_e computed data could produce different transition onset predictions when applied at flight conditions using either the LATCH or the LAURA flight data sets.

Concluding remarks

Orbiter boundary layer properties from viscous CFD solutions were compared along the wind side centerline against results from a two-layer boundary layer prediction tool. The two-layer tool couples inviscid CFD with an approximate boundary layer solver.

As verification of the viscous CFD results, grid convergence of the boundary layer transition parameter $\left(\frac{Re_\theta}{M_e}\right)\cdot\left(\frac{1}{\delta}\right)$ was checked and observed to be within 5% relative to a 50% increase, from 64 to 96 cells, in grid resolution from the surface to the far field boundary. Also, results from two different viscous CFD codes, LAURA and DPLR, were compared at flight Mach 18 and 20 conditions. Agreement between the codes for boundary layer edge properties is on the order of 10%.

The relationship between the viscous CFD and two-layer results is not consistent between Mach 6 wind tunnel and Mach 6 flight simulations. Similarly, the relationship between the viscous CFD and two-layer results is not consistent between Mach 6 and Mach 18 flight conditions. The differences between the viscous CFD and two-layer results are as much as 30%. A straightforward mapping or scaling of the approximate boundary layer prediction methodology to the viscous CFD results is not readily apparent.

The viscous CFD solutions are recommended to be suitable for the development of boundary layer transition correlations. But it does not appear that the existing two-layer boundary layer results can be leveraged in the development of the necessary tunnel and flight data sets, due to the inconsistency in boundary layer prediction trends between the two-layer and viscous CFD data.

Acknowledgments

Some of the LAURA solutions were provided by Dr. Peter Gnoffo of Langley Research Center. The DPLR solutions were provided by Dr. Dinesh Prabhu and Dr. David Saunders of Eloret Corporation.

David Erickson was supported through the Langley Aerospace Research Summer Scholars program.

References

1. Berry, S. A.; Horvath, T. J.; Greene, F. A.; Kinder, G. R.; and Wang, K. C.: Overview of Boundary Layer Transition Research in Support of Orbiter Return to Flight. AIAA Paper 2006-2918, June 2006.

2. Greene, F. A.; and Hamilton, H. H.: Development of a Boundary Layer Properties Interpolation Tool in Support of Orbiter Return to Flight. AIAA Paper 2006-2920, June 2006.

3. Hamilton II, H. H.; Greene, F. A.; and DeJarnette, F. R.: Approximate Method for Calculating Heating Rates on Three-Dimensional Vehicles. *Journal of Spacecraft and Rockets*, vol. 31, no. 3, May 1994, pp. 345–354.

4. External Aerothermal Analysis Team: Smooth Outer Mold Line Aerothermal Solution Database for Orbiter Windside Acreage Environments During Nominal Entry Conditions. Engineering Note EG-SS-06-1, NASA Johnson Space Center, Houston, Texas, Apr. 2005. Presented to Orbiter Configuration Control Board.

5. Gnoffo, P. A.; Gupta, R. N.; and Shinn, J. L.: Conservation Equations and Physical Models for Hypersonic Air Flows in Thermal and Chemical Nonequilibrium. NASA TP 2867, Feb. 1989.

6. Gnoffo, P. A.: An Upwind-Biased, Point-Implicit Relaxation Algorithm for Viscous, Compressible Perfect-Gas Flows. NASA TP 2953, Feb. 1990.

7. Wright, M. J.; Candler, G. V.; and Bose, D.: Data-Parallel Line Relaxation Method for the Navier-Stokes Equations. *AIAA Journal*, vol. 36, no. 9, Sept. 1998, pp. 1603–1609.

8. Bertin, J. J.: *Hypersonic Aerothermodynamics*. Education Series, AIAA, Washington, DC, USA, 1994.

9. Saunders, D.; and Prabhu, D.: Curvature-Based Boundary Layer Edge Detection. In preparation, Eloret Corporation, 2007.

10. Berry, S. A.; Hamilton, H. H.; and Wurster, K. E.: Effect of Computational Method on Discrete Roughness Correlations for Shuttle Orbiter. *Journal of Spacecraft and Rockets*, vol. 43, no. 4, July 2006, pp. 842–852.

REPORT DOCUMENTATION PAGE

Form Approved
OMB No. 0704–0188

1. REPORT DATE *(DD-MM-YYYY)*	2. REPORT TYPE	3. DATES COVERED *(From - To)*
01-06-2007	Technical Memorandum	

4. TITLE AND SUBTITLE
Orbiter Entry Aeroheating Working Group viscous CFD boundary layer transition trailblazer solutions

5a. CONTRACT NUMBER

5b. GRANT NUMBER

5c. PROGRAM ELEMENT NUMBER

6. AUTHOR(S)
William A. Wood, David W. Erickson, and Francis A. Greene
Langley Research Center, Hampton, Virginia

5d. PROJECT NUMBER

5e. TASK NUMBER

5f. WORK UNIT NUMBER

7. PERFORMING ORGANIZATION NAME(S) AND ADDRESS(ES)
NASA Langley Research Center
Hampton, Virginia 23681-2199

8. PERFORMING ORGANIZATION REPORT NUMBER
L–19281

9. SPONSORING/MONITORING AGENCY NAME(S) AND ADDRESS(ES)
National Aeronautics and Space Administration
Washington, DC 20546-0001

10. SPONSOR/MONITOR'S ACRONYM(S)
NASA

11. SPONSOR/MONITOR'S REPORT NUMBER(S)
NASA/TM–2007–214882

12. DISTRIBUTION/AVAILABILITY STATEMENT
Unclassified-Unlimited
Subject Category 34
Availability: NASA CASI (301) 621-0390

13. SUPPLEMENTARY NOTES
An electronic version can be found at http://ntrs.nasa.gov.

14. ABSTRACT

Boundary layer transition correlations for the Shuttle Orbiter have been previously developed utilizing a two-layer boundary layer prediction technique. The particular two-layer technique that was used is limited to Mach numbers less than 20. To allow assessments at Mach numbers greater than 20, it is proposed to use viscous CFD to the predict boundary layer properties. This report addresses if the existing Orbiter entry aeroheating viscous CFD solutions, which were originally intended to be used for heat transfer rate predictions, adequately resolve boundary layer edge properties and if the existing two-layer results could be leveraged to reduce the number of needed CFD solutions. The boundary layer edge parameters from viscous CFD solutions are extracted along the wind side centerline of the Space Shuttle Orbiter at reentry conditions, and are compared with results from the two-layer boundary layer prediction technique. The differences between the viscous CFD and two-layer prediction techniques vary between Mach 6 and 18 flight conditions and Mach 6 wind tunnel conditions, and there is not a straightforward scaling between the viscous CFD and two-layer values. Therefore: it is not possible to leverage the existing two-layer Orbiter flight boundary layer data set as a substitute for a viscous CFD data set; but viscous CFD solutions at the current grid resolution are sufficient to produce a boundary layer data set suitable for applying edge-based boundary layer transition correlations.

15. SUBJECT TERMS
Orbiter, RTF, boundary layer

16. SECURITY CLASSIFICATION OF:			17. LIMITATION OF ABSTRACT	18. NUMBER OF PAGES	19a. NAME OF RESPONSIBLE PERSON
a. REPORT	b. ABSTRACT	c. THIS PAGE			STI Help Desk (email: help@sti.nasa.gov)
U	U	U	UU	22	19b. TELEPHONE NUMBER *(Include area code)* (301) 621-0390